Radiocarbon, Vol 61, Nr 6, 2019, p 1805–1812 DOI:10.1017/RDC.2019.118
Selected Papers from the 23rd International Radiocarbon Conference, Trondheim, Norway, 17–22 June, 2018
© 2019 by the Arizona Board of Regents on behalf of the University of Arizona

ION-PAIR IONIZATION IN CO_2-FED CESIUM SPUTTER SOURCES

John S Vogel[1]* • Alexander M Stolz[2]

[1]University of California (retired); 8300 Feliz Creek Dr., Ukiah, CA 95482, USA
[2]Institut für Kernphysik; Universität zu Köln; Zülpicher Str. 77, 50937 Köln DE, Germany

ABSTRACT. A collision-radiation model of the solid sample cesium sputter ion source led to the rediscovery of anion production by ion-pair production. The model revealed physical processes that may produce high current outputs from such sources and suggested new ways of obtaining high outputs at lower heat and conductive stress to the source. Primary among these solutions is the electron excitation of primary Cs^0 recycled from the sample to provide states that efficiently create chosen anions. Here we look at how the processes might apply to gas-fed ion sources.

KEYWORDS: gas-fed ion source, ion-pair, ionization.

INTRODUCTION

Statistically precise radiocarbon accelerator mass spectrometry (^{14}C AMS) measurements require high count-rates of ^{14}C from the cesium sputter anion source. One carbon is sputtered from solid carbon for every incident Cs of 8–10 keV (Yamamura and Tawara 1996). However, surface effects ionize less than 3% of these sputtered atoms (Litherland et al. 1987). Creation of elemental anions through ion-pair production (IPP) during collisions of neutral sputtered products with neutral gaseous cesium (Cs) in ground or excited states is suggested to be much more efficient than surface ionization for Cs sputter ion sources (Vogel 2013, 2015, 2016, 2018; Vogel et al. 2013). Sputtered atoms come off a surface with a energy distribution maximizing at half their binding energy (BE) (Sigmund 1969). The BE of fullerene carbon atoms is 8.8 eV (Porezag et al. 1995) and that of Cs to Cs is 2.31 eV (Kudriatsev et al. 2005), predicting less than 4.4 eV C^0 and 1.15 eV Cs^0 in the ionizing collision. The sputter region is ≈ 500–700° K (above the bulk Cs sublimation at 300° K) yielding a larger evaporated fraction of Cs at 60 meV thermal energy. Thus, the maximum center of mass collision energy for C^0-Cs^0 is around 5 eV, a collision energy too low for well known ionization mechanisms (Middleton and Klein 1999).

Our search for a low-energy mechanism of electron transfer began with a collision-radiation model (CRM) of neutral Cs evaporated from a solid sample of carbon under the influence of secondary sputtered electrons (SSE) (Vogel 2013). The CRM showed that SSE were indeed capable of exciting Cs to the 7d excited state and beyond, easily producing the 7p state which decays to the ground state, emitting the characteristic 455.7 and 459.4 nm blue light observed above the sample in intense Cs sputter ion sources (Middleton and Klein 1999) Andersson et al. (2013) spectroscopically confirm that the plasma above C and Al samples emit these Cs(7p) lines. These 7p states of Cs have ionization potentials (IP) of 1.195 and 1.173 eV, close to the 1.263 eV electron affinity (EA) of carbon. The intense beams of C^- that are noted when the blue plasma is present above a graphite sample were first thought to be related to a near resonant transfer of the excited electron to the anion (Vogel 2015). The search for a resonant process at this low energy, however, led to a rediscovery of the ion-pair process (IPP). IPP was discovered by Lee and Mahan (1965) in an irradiated thermal Cs vapor causing a collision between a Cs atom and an excited Cs atom to produce negative ions: $Cs+Cs^* \rightarrow Cs^+ + Cs^-$. Beam collision instruments explored molecular negative ion production in alkali collisions through the 1970s (Baede et al. 1969) and this chemical application

*Corresponding author. Email: johnsvogel@yahoo.com.

https://doi.org/10.1017/RDC.2019.118 Published online by Cambridge University Press

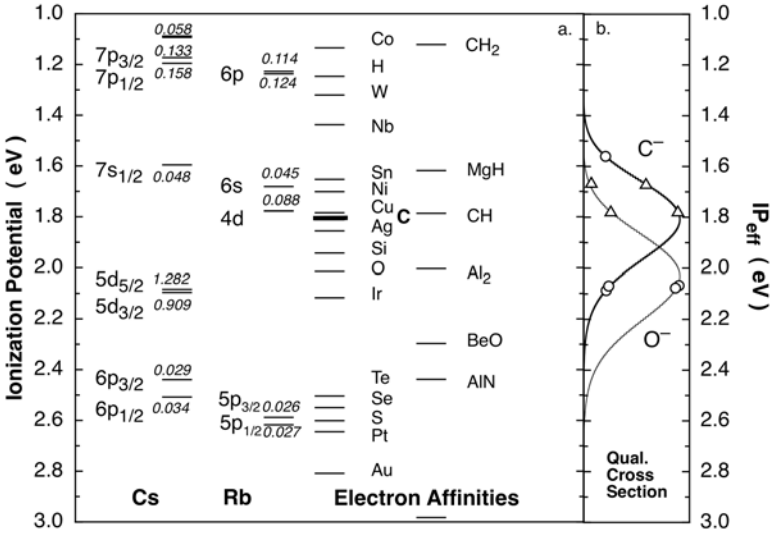


Figure 1 a. Excited states of cesium and rubidium are plotted versus their ionization energies, with their mean lives noted above or below their positions in μsec. The effective ionization potentials for anion creation of selected elements and molecules through IPP collisions are shown to the right, centered on carbon (Desfrançois 1995). b. Qualitative cross sections that we derived for C^- and O^- are shown as continuous variables with their relative magnitudes at excited states as circles (Cs) and triangles (Rb). Oxygen dominates at the metastable Cs*(5d) states. A shift to Rb+ primary ions gives that dominance to C, but without the advantage of metastable states.

continues to the present (Ciborowski et al. 2018). Physics was less interested in IPP, with only 2 explorations for elemental anions from collisions of excited atoms: $Rb+Rb^*\rightarrow Rb^+ + Rb^-$ (Barbier et al. 1986) and $Ca+Ne^*\rightarrow Ne^+ + Ca^-$ (Reicherts et al. 1997).

IPP is a chemi-ionization in which the energy is supplied partly by chemical excitation in atoms or molecules, similar to Penning or Associative ionization. However, even recent articles about chemi-ionization refrain from describing IPP, emphasizing the other two processes (Klyucharev 1993; Mihajlov et al. 2012). Working from a semi-classical description of the Ca on Ne* reaction by Buslov and Zon (2012), we derived a description of IPP providing the optimal excitation for any electron donor element in collisions creating anions from any element having a positive electron affinity (Vogel 2018) While the electron transfer is nearly resonant between halogens and ground state alkalis explored in the 1970s, the reaction overall is endoergic, requiring a kinetic input up to 0.5 eV for making the oxygen anion, for example.

Our effort heretofore emphasized means of obtaining higher sputtered anion currents from solid samples while decreasing anions of isobar elements. Given the wide interest in increasing C^- from CO_2-fed ion sources evidenced at AMS-14 in Ottawa, our paper there was modified to consider the problematic overlap of the C and the O atoms obtaining their primary ionizations from the copious metastable Cs*(5d) state (Vogel 2018). An offered solution was to change the primary sputter ion to Rb^+, which favors the C anion over the O anion, as seen in Figure 1. While there is evidence that this change of primary ion is not overly radical (Lachner et al. 2015) few may be ready to turn their backs on decades of experience with Cs.

https://doi.org/10.1017/RDC.2019.118 Published online by Cambridge University Press

In this paper, we consider the recent successes of CO_2-fed sources in obtaining C^- currents as high as 20 μA in light of the IPP theory (Xu et al. 2007; Fahrni et al. 2013; Stolz et al. 2017, 2018).

CESIUM EXCITATION

Cesium has the most easily excited valence electron, with the first excited state (6p) only 1.4 eV above the ground state (6s). This 6s-6p pair constitute a resonance, such that at sufficient atomic density, the photon released by a decaying Cs(6p) is likely to collide with a Cs(6s), exciting it to a new Cs(6p). This stable resonance platform provides the basis for a decreasing step-wise ladder of _electron excitation energies to any higher state, including ionization. SSE from Cs^+ sputtering of conductors and semiconductors produces one electron per primary ion with a maximum energy between 1 and 3 eV, well suited to provide such initial and subsequent electron excitations to Cs (Krebs 1983; Avilkina et al. 2011). Electrons have a high elastic scattering cross section with Cs (≈150 $Å^2$) below the excitation threshold at 1.39 eV (Zecca et al. 1996) and scatter until absorbed by a Cs excitation or the well wall. Thus, the ionizing potential of excited Cs states in sputter sources for carbon depends on obtaining Cs^0 gas densities that maintain a populated Cs(6p) state or on sufficient electron emissions at energies that excite the long lived Cs(5d) state at 1.8 eV.

We used a CRM to explore excitation versus Cs^0 densities (Vogel 2013). The CRM was implemented in a linear differential equation solver (Berkeley Madonna, Berkeley CA) with constant electron and photon excitation rates derived from numerical integrals of cross sections against expected fluxes. Following presentation at a negative ion source meeting, this CRM structure was expanded in detail to investigate Cs^0 excited states in RF ion sources for use in driving and probing ITER (Wünderlich et al. 2014; Priti et al. 2017). The Cs and electron densities in these are too low for useful comparisons. Our modeled physical process included accepting all primary Cs^+ ions focused into a 1 mm × 1 mm cylindrical well in a metal sample holder with a solid sample at the bottom. The rate of primary ions sputtering the sample was taken from the current of the cathode potential set off from the ionizer, which was of the order of 1 mA, or 6.2×10^{15} ions/sec. Sputtered secondary atoms number 1 (C) to 10 (Cu) per primary (Yamamura and Tawara 1996). SSE also number one electron per Cs primary from conductive targets at typical sputter energies (8–12 keV) (Krebs 1983; Avilkina et al. 2011), but are partially deflected from extraction by source-mounted magnets. Depending on source optical elements and power supplies, an electron current is read from the extraction supply to correct the cathode current for electron contributions. Of the embedded primary Cs^+, ≈10% is re-sputtered by incoming Cs^+ while >80% evaporate from the hot surface at less than 0.06 eV energy (Vandervorst et al. 2008). Less than 10% is retained in the sample. Cs^0 at thermal energy exits a 1 mm well depth in ≈3 μsec rms time, leaving approximately 9×10^9 Cs in the 0.78×10^{-9} m^3 well, for a density of $\approx 1 \times 10^{19}$ /m^3, a density sufficient for resonance of 6s-6p states and shown in Figure 2 as a long line at the left marked "A". The Cs^0 gas continues as a semi-collimated beam at the sample well top, of course, while the CRM incorporates an abrupt halt of SSE excitation at the well edge (Vogel 2016).

GAS-FED ION SOURCES

Electron excitation of the Cs^0 states for IPP is not as certain for gas-fed sources as solid sample sources, given the more complex sputtering environment of C and O absorbed onto the Ti lattice and the presence of the helium carrier/buffer gas amid the sputtered products. Thus, the following ideas may be considered speculation that reveals experiments to be tried and

https://doi.org/10.1017/RDC.2019.118 Published online by Cambridge University Press

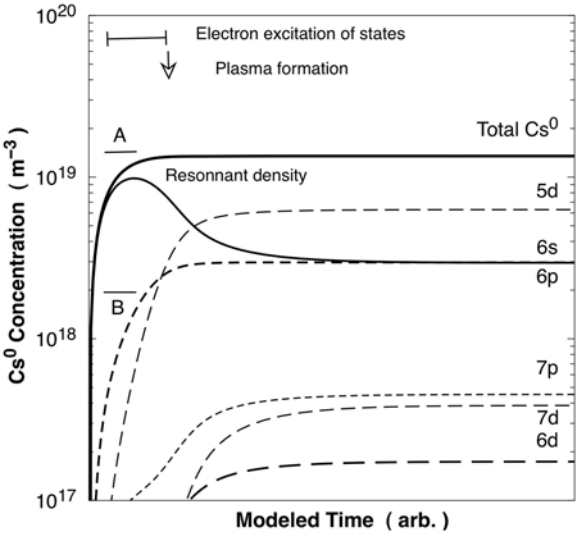


Figure 2 Densities of the excited states of Cs versus modeled time for a chosen total input of C. The origin of the resonant pair around 10^{19} Cs/m^3 leads to Cs(6p) equalling Cs(6s), with Cs(5d) dominant The Cs^0 density for our modeled solid graphite sample (line A) is in this resonance. Line B represents the Cs density of the U. Köln CO_2-fed ion source and is below resonance.

models to be constructed. Once Middleton (1984) revealed the gas-fed sputter source concept, development was slow, with only Oxford exploring the use in the 1980s (Bronk and Hedges 1987), Ruff et al. (2007), Uhl et al. (2007), Xu et al. (2007), and Stolz et al. (2017), among others, have since developed the capability. The general assumption is that the C and the O are captured on/into the Ti lattice as TiC and TiO_2, while He carrier gas flows through the sample area to vacuum. The Ti anvils take various forms, from bars to conical pits, but are recessed where the Cs gas excitation by SSE can occur. Uhl et al. (2004, 2007) and Xu et al. (2007) describe gas modifications of NEC ion sources, which do not easily allow visual inspection for blue Cs plasma at the sample. Xu et al. (2007) demonstrate robust C^- with pure CO_2 feed, but do not provide their Cs boiler temperatures or the measured ionizer-cathode current, so an estimate of Cs gas density in front of the sample anvil cannot be made.

Fahrni et al. (2013) describe an improved Cs sputter ion source used on the MICADAS™ instruments from IonPlus™ that uses 15 keV Cs^+ primary from boilers at 150–185°C to attain ⁻high currents. At a 1 mA Cs^+ current, this source surely operates in the SSE-excited plasma mode, and the characteristic blue light is reportedly visible above the Ti anvil. The biggest difficulty in operating the source at high boiler temperatures is the rapid build-up of conductive Cs on source structures and the plugging of gas channels, as the authors note. Resonant density for electronic excitation of Cs is probably attained in the apparent small "well" shown in their Figure 4. The opening diameter of the Al holder is stated at 1.1 mm and the thickness of the Al holding the Ti anvil appears to be 1 mm thick, making the well similar in size to that modeled in our CRM.

Data from the Köln AMS Laboratory recently showed that a SO-110B CO_2-fed ion source from HVE produced 10% more carbon anions if the Cs^0 vapor in front of the Ti anvil were

https://doi.org/10.1017/RDC.2019.118 Published online by Cambridge University Press

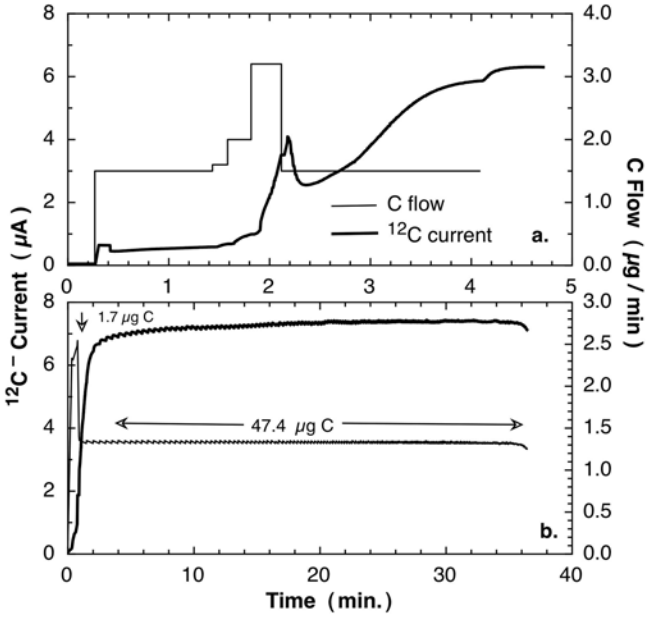


Figure 3 a. The CO_2-fed HVEE S011B has initial negative ion current of < 2 μA at carbon flow of 1.5 μg/min. Doubling flow for 20–60 seconds, triggers another mode in which the source outputs 6–12 μA. b. The high output continues for long periods. Doubling C flow requires only 1–2 μg C to attain increased anion current. A "sawtooth" pattern arises from the gas syringe for this pure CO_2 sample (Stolz 2020).

exposed to 450 nm laser light, very weakly exciting the Cs*($7p_{3/2}$) state (Stolz et al. 2018). This replicated results from a graphite sputter source (Vogel and Giacomo 2016) and suggested that this gas fed source ionizes by IPP. This source also produces up to 400μA C^- from fullerene graphite (Klein and Mous 2017) which indicates that it normally ionizes solid samples by IPP, since that current is unavailable from surface ionization. The gas source exhibits 2 states of C^- emission, however, one at the low 1–3 μA levels shown by many CO_2-fed sources, and another at higher 6–12μA output, both occurring with ≈ 0.4 mA primary current. The lower output is assumed due to surface ionization of C captured on the Ti anvil. This flux is accompanied by O^- at twice the C^- current. The higher output, presumably by IPP from excited states of neutral Cs, is achieved in this source by a momentary doubling of the gas feed, as seen in Figure 3a. This "pulse" of sample gas uses a small fraction of the carbon sample, but the higher ion current continues for long periods, as seen in Figure 3b where the measured sample size totals 49.1 μg. The gas control is programmed to provide this igniting "squirt" for each sample, maintaining the increased gas flow until the rise in sample current is detected. The "ignition" occurs in tens of seconds using 1–2 μg of sample CO_2, which is acceptable except for very small samples (≤3 μg). The mechanism for this change is mysterious. We have considered, without satisfaction, two possible causes: modification of the Ti anvil surface and an increase in electron density due to added gas among the neutral Cs.

Clean metal and semiconductor surfaces produce 0.5–1 sputtered electron per incident monatomic ion at 8–10 keV (Krebs 1983). Our CRM for solid graphite assumed production of 1 electron from carbon per ion, as found by others (Cernusca et al. 2005; Avilkina et al. 2011).

https://doi.org/10.1017/RDC.2019.118 Published online by Cambridge University Press

The oxides of Be and Al, both insulators, emit 5–7 SSE per 10 keV sputter ion (Dietz and Sheffield 1975), although Stein and White (1972) found only 3 SSE per 10 keV ion for Al_2O_3 and for TiO_2. Stein and White's oxide layer on titanium was only the naturally occurring oxide found on cold-rolled, 99% pure Ti foil. No other directly applicable data was found, and we adopt an electron yield of 3 from the explicit measure of TiO_2. Multiple gases getter on Ti (Stout and Gibbons 1955), with CO and CO_2 (but not CH_4) dissociating on clean Ti surfaces (Carrillo et al. 2015). The same authors show through theoretical chemistry that CO_2 dissociates to CO and O on clean Ti, but, surprisingly, the resultant CO remains stable since the nearby surface is oxidized rather than "clean."

Electron excitation of Cs states comes from SSE that are emitted in a pseudo-Boltzmann distribution maximizing at 2–3 eV (Krebs 1983) from sputtered metals. Electrons emitted from insulators extend to higher energies, peaking above the Cs ionization energy at 4 eV, due to plasmon and Auger mechanisms (Ruano et al. 2011). This means that the Cs^0 cloud in front of the Ti anvil receives three times (and perhaps more) the electron flux as modeled for a solid graphite samples, including a higher fraction of ionizing electrons. Electrons from sputtered insulators require a new model structure, which we are initiating. Our CRM is no longer available due to changes in computer hardware. The cross sections for 2 eV secondary electrons on Cs^0(6s) to Cs^0(6p) and on Cs^0(6p) to Cs^0(5d) are 30 $Å^2$ and 300 $Å^2$, dominating the stepwise excitation in a solid ion source, while higher energy electrons promote Cs^0(6s) to Cs^0(5d) at 3 $Å^2$ cross section (Priti et al. 2017). Thus, paths to the Cs(5d) state that ionizes the C atom are probable at higher electron energies with the lower Cs densities of gas ion sources without involving the blue plasma from excitation to the Cs(7p) state. We suspect that the low output from the gas ion source results from lower Cs density and these less favorable excitations to the Cs(5d) state. The doubling of gas flow shown in Figure 3 may increase the oxygen flow to the Ti anvil, decreasing the time needed to build up a sufficient insulating TiO_2 layer to sustain the electron emission. However, continued low-flow sample delivery should eventually provide equivalent oxide insulation and higher output, which is not seen.

Cesium has a density in the Köln sample well of $\approx 2 \times 10^{18}$ Cs/m^3. This density is below the 6s-6p resonance, as marked by the line B in Figure 2, preventing the step-wise excitation of higher states as seen in the solid sample model. Further, the Cs(7p) blue plasma is not seen in this source. SSE below the 1.4 eV inelastic threshold to Cs(6p) scatter from the Cs^0 gas with a large elastic cross section of 150$Å^2$ until loss or excitation between close states occurs. Elastic scatter off Cs affects only ≈0.9% of the electrons within the sample well, however. Dilution of the sample CO_2 to 5% in helium gas is the normal mode of operation to conserve small samples. Helium also adds elastic electron scattering, with a 6 $Å^2$ cross section below 10 eV (Zecca et al. 1996), but the He adds only 0.8% elastic scatter to that of Cs. The data in Figure 3 came from 100% CO_2 samples, demanding yet further investigation. One is tempted to assume that all of the CO_2 interacts with the Ti anvil, but the complete detection efficiency of <7% shows otherwise. Thus, the sample well also contains CO_2, CO, C, and O whose elastic scattering of 2–5 eV electrons are 10, 40, 10, and 8 $Å^2$, respectively (Thomas and Nesbet 1975; Zecca at al. 1996; Szmytkowski and Maciqg 1996; Itikawa 2002). The doubling of the gas flow could add to the electron densities exciting the Cs, but the contributions from each are 1% or lower. These contributions to the additional electron densities appear too low for significance, but a detailed collision-radiation-model for these interactions is needed for further inspiration.

This analysis is hypothetical, based on descriptions of the S011B ion source and a targeted literature search for means of exciting Cs(5d) at Cs densities below resonance. Experiments

https://doi.org/10.1017/RDC.2019.118 Published online by Cambridge University Press

to test the hypotheses include modifications of the Ti surface, but they may be difficult since Ti oxidizes so rapidly in air. We will test a 460 nm laser to excite the Cs(7p) state which decays to provide significant long-lived Cs(5d) in the neutral gas at the top of the sample well. Such application of optical excitation is expected to be more efficient than hypothesized electron excitation.

CONCLUSION

We compared our CRM analysis of cesium sputter-source operation for solid carbon samples to examples of CO_2-fed Cs sputter sources. In one case, increased C^- is found for high concentrations of Cs input that are disruptive to reliable routine operations. Lower Cs boiler temperatures for the Köln gas fed source revealed other hypothetical paths to obtaining sufficiently excited Cs^0 gas in front of the samples for ion-pair ionization to proceed. These divergent techniques present alternatives to our initial suggestion of using a Rb primary beam in CO_2-fed sources (Vogel 2018), but still support the use of laser excitation of the Cs in a gas-fed ion source.

REFERENCES

Andersson P, Martschini M, Priller A, Steier P, Golser R, Forstner O. 2013. Spectroscopic analysis of the blue light emitted from Middleton type cesium sputter negative ion sources. Nuclear Instruments and Methods in Physics Research B 295:55–60.

Avilkina V, Andrianova N, Borisov A, Mashkova E, Parikis E. 2011. Energy and temperature dependence of ion-induced electron emission from polycrystaline graphite. Nuclear Instruments and Methods in Physics Research B 269:995–998.

Baede APM, Moutinho AMC, De Vries AE, Los J. 1969. Total cross sections for charge transfer between alkali atoms and halogen molecules. Chemical Physics Letters 3(7):530–531.

Barbier L, Djerad MT, Chéret M. 1986, Collisional ion-pair formation in an excited alkali-metal vapor. Physical Review A 34(4):2710.

Bronk CR, Hedges REM. 1987. A gas ion source for radiocarbon dating. Nuclear Instruments and Methods in Physics Research B 29:45.

Buslov E, Zon BA. 2012. Formation of negative ions in collisions between Rydberg atoms and neutral particles. Physical Review A:85(4).

Carrillo I, Ramirez JM, Magaña LF. 2015. Adsorption of carbon monoxide, carbon dioxide and methane on hexagonal boron nitride with high titanium coverage. Surface Science. 637–638:48–52.

Cernusca S, Fürsatz M, Winter HP, Aumayr F. 2005. Ion-induced kinetic electron emission from HOPG with different surface orientation. Europhysics Letters 70:768.

Ciborowski SM, Liu G, Graham JD, Buytendyk AM, Bowers KH. 2018. Dipole-bound anions: formed by Rydberg electron transfer (RET) and studied by velocity map imaging–anion photoelectron spectroscopy (VMI–aPES). Eur. Phys. Jour. D 72:139.

Desfrancois C. 1995. Determination of electron binding energies of ground-state dipole-bound molecular anions. Physical Review A 51(5): 3667–3675.

Dietz LA, Sheffield JC. 1975. Secondary electron emission induced by 5–30-keV monatomic ions striking thin oxide films. Journal of Applied Physics 46:4361.

Fahrni SM, Wacker L, Synal H-A, Szidat S. 2013. Improving a gas ion source for ^{14}C AMS. Nuclear Instruments and Methods in Physics Research B 294:320–327.

Itikawa Y. 2002. Cross sections for electron collisions with carbon dioxide. J. Phys. Chem. Ref. Data. 31: 749.

Klein M, Mous DJW. 2017. Technical improvements and performance of the HVE AMS sputter ion source SO-110. Nuclear Instruments and Methods in Physics Research B 406:210.

Klyucharev A. 1993. Chemi-ionization processes. Physics Uspekhi 36:486.

Krebs KH. 1983. Recent advances in the field of ion-induced kinetic electron emission from solids. Vacuum 33:555.

Kudriatsev Y, Villegas A, Godines A, Asomoza R. 2005. Calculation of the surface binding energy for ion sputtered particles. Appl. Surf. Sci. 239: 273–278.

Lachner J, Kasberger M, Martschini M, Priller, A, Steier P, Golser R. 2015. Developments towards detection of ^{135}Cs at VERA. Nuclear Instruments and Methods in Physics Research B 361(C): 440–444.

Lee YTT, Mahan BH. 1965. Photosensitized ionization of alkali-metal vapors. The Journal of Chemical Physics 42(8):2893–2896.

Litherland AE, Paul M, Allenc KW, Gove HE. 1987. Fundamentals of accelerator mass spectrometry [and Discussion]. Phil. Trans. R. Soc. London A 323:5–21.

https://doi.org/10.1017/RDC.2019.118 Published online by Cambridge University Press

Middleton R. 1984. A versatile high intensity negative ion source. Nuclear Instruments and Methods in Physics Research 220:105.

Middleton R, Klein J. 1999. Production of metastable negative ions in a cesium sputter source: Verification of the existence of N_2^- and CO^-. Physical Review A 60(5):3786.

Mihajlov AA, Srećković VA, Ignjatović LM, Klyucharev AN. 2012, The chemi-ionization processes in slow collisions of Rydberg atoms with ground state atoms: mechanism and applications, Journal of Cluster Science 23(1):47–75.

Porezag D, Frauenheim T, Köhler T, Seifert G, Kaschner R. 1995. Construction of tight-binding-like potentials on the basis of density-functional theory: Application to carbon. Physical Review B 51(19):12947.

Priti D, Gangwar RK, Srivastava R. 2017. Calculation of fully relativistic cross sections for electron excitation of cesium atom and its application to the diagnostics of hydrogen-cesium plasma. Journal of Qualitative Spectroscopy and Radiation Transfer 187:426.

Reicherts M, Roth T, Gopalan A, Ruf MWW, Hotop H, Desfrançois C, Fabrikant II. 1997. Controlled formation of weakly bound atomic negative ions by electron transfer from state-selected Rydberg atoms. EPL (Europhysics Letters) 40(2):129.

Ruano G, Vidal RA, Ferron J, Baraguiola RA. 2011. High energy excitations in ion-induced electron enission from AlF_3. Surface Science 605: 1807–1811.

Ruff M, Wacker L, Gäggler HW, Suter M. 2007. A gas ion source for radiocarbon measurements. Radiocarbon 49:307.

Sigmund P. 1969, Theory of sputtering. I. Sputtering yield of amorphous and polycrystalline targets. Physical Review 184:383.

Stein JD and White FA. 1972. New method for the measurement of electron yield from ion bombardment. Jour. Applied Physics 43:2617.

Stolz A. 2020. Einrichtung und Weiterentwicklung eines $^{14}CO_2$-Systems am 6 MV TANDETRON Beschleuniger des CologneAMS [Ph.D. thesis]. Cologne: University of Cologne. 112 p

Stolz A, Dewald A, Altenkirch R, Herb S, Heinze S, Schiffer M, Feuerstein C, Muller-Gatermann C, Wotte A, Rethemeyer J, Dunai T. 2017. Radiocarbon measurements of small gaseous samples at Cologne AMS. Nucl. Instr. and Meth. B 406: 283–286.

Stolz A, Dewald A, Heinze S, Altenkirch R, Hackenberg G, Herb S, Muller-Gatermann C, Schiffer M, Zitzer G, Wotte A, Rethemeyer J, Dunai T. 2018. Improvements in the measurement of small $^{14}CO_2$ samples at Cologne AMS. Nuclear Instruments and Methods in Physics Research B. In press.

Stout VL, Gibbons MD. 1955. Gettering of gas by tiyanium. Journal of Applied Physics 26:1488.

Szmytkowski C. and Maciqg K. 1996. Absolute electron-scattering totaI cross section measurements for noble gas atoms and diatomic molecules. Physica Scripta 54: 271–280.

Thomas LD, Nesbet RK. 1975. Low energy electron scattering by atomic carbon. Phys. Rev. A 12:2378–2382.

Uhl T, Kretschmer W, Luppold W, Scharf A. 2004. Direct coupling of an elemental analyzer and a hybrid ion source for AMS measurements. Radiocarbon 46:65.

Uhl T, Luppold W, Rottenbach A, Scharf A, Kretschmer W. 2007. Development of an automatic gas handling system for microscale AMS ^{14}C measurements. Nuclear Instruments and Methods in Physics Research B 259:303.

Vandervorst W, Janssens T, Huyghebaert C, Berghmans B. 2008. The fate of the (reactive) primary ion: Sputtering and desorption. Applied Surface Science 255:1206–1214.

Vogel JS. 2013. Neutral resonant ionization in the high-intensity cesium sputter source. In: Third International Symposium on Negative Ions, Beams and Sources. AIP Conference Series 1515:89–98.

Vogel JS, Giacomo JA, Dueker SR. 2013. Quantifying absolute carbon isotope ratios by AMS. Nuclear Instruments and Methods in Physics Research B 294:340–348.

Vogel JS. 2015. Anion formation by neutral resonant ionization. Nuclear Instruments and Methods in Physics Research B 361:156–62.

Vogel JS. 2016. Anion formation in sputter ion sources by neutral resonant ionization. Review of Scientific Instruments 87:02A504.

Vogel JS, Giacomo JA. 2016. Increased ^{14}C AMS efficiency from reduced competitive ionization. Radiocarbon. doi: 10.1017/RDC.2016.38.

Vogel JS. 2018. LASIS: the laser assisted sputter ion source. Nuclear Instruments and Methods in Physics Research B. doi: 10.1016/j.nimb.2018.07.015

Submitted Vogel-Stolz Manuscript Wünderlich D, Wimmer C, Friedl R. 2014. A collisional radiative model for low-pressure hydrogen–caesium plasmas and its application to an RF source for negative hydrogen ions. Journal of Qualitative Spectroscopy and Radiation Transfer 149:360.

Xu S, Dougans A, Freeman SPHT, Maden C, Loger R. 2007. A gas ion source for radiocarbon measurement at SUERC. Nuclear Instruments and Methods in Physics Research B 259:76.

Yamamura Y, Tawara H. 1996. Energy dependence of ion-induced sputtering yields from monatomic solids at normal incidence. Atomic Data and Nuclear Data Tables 62:2

Zecca A, Karwasz P, Brusa RS. 1996. One century of experiments on electron-atom and molecule scattering: a critical review of integer cross-sections. Rivista del Nuovo Cimento 19(3):1.

https://doi.org/10.1017/RDC.2019.118 Published online by Cambridge University Press